Published in final edited form as:
Neuron. 2011 September 8; 71(5): 799–811. doi:10.1016/j.neuron.2011.07.022.

Development of a Novel Method for the Purification and Culture of Rodent Astrocytes

Lynette C. Foo[1,*], **Nicola J. Allen**[1], **Eric A. Bushong**[3], **P. Britten Ventura**[4], **Won-Suk Chung**[1], **Lu Zhou**[1], **John D. Cahoy**[1], **Richard Daneman**[2], **Hui Zong**[4], **Mark H. Ellisman**[3], and **Ben A. Barres**[1]

[1]Stanford University School of Medicine, Department of Neurobiology, Stanford CA

[2]Department of Anatomy, University of California San Francisco, San Francisco CA

[3]National Center for Microscope and Imaging Research, University of California at San Diego, La Jolla, CA

[4]Institute of Molecular Biology, University of Oregon, Eugene, OR

Summary

The inability to purify and culture astrocytes has long hindered studies of their function. Whereas astrocyte progenitor cells can be cultured from neonatal brain, culture of mature astrocytes from postnatal brain has not been possible. Here we report a new method to prospectively purify astrocytes by immunopanning. These astrocytes undergo apoptosis in culture, but vascular cells and HBEGF promote their survival in serum-free culture. We found that some developing astrocytes normally undergo apoptosis *in vivo* and that the vast majority of astrocytes contact blood vessels, suggesting that astrocytes are matched to blood vessels by competing for vascular-derived trophic factors such as HBEGF. Compared to traditional astrocyte cultures, the gene profiles of the cultured purified postnatal astrocytes much more closely resemble those of *in vivo* astrocytes. Although these astrocytes strongly promote synapse formation and function, they do not secrete glutamate in response to stimulation.

Introduction

Astrocytes are a major cellular constituent of the central nervous system (CNS) outnumbering neurons in humans (Nedergaard et al, 2003). Long thought to play primarily passive support roles in the nervous system, recent evidence has highlighted their importance in the formation, function, and elimination of synapses (Eroglu and Barres, 2010). Despite these advances, our understanding of astrocyte development and function, and their signaling interactions with other cell types both in health and disease, is still rudimentary.

As neurons are reliant on astrocyte-derived trophic support, the functions of astrocytes with respect to neurons cannot be uncovered merely by deleting them. However, progress in understanding astrocyte biology has been stymied by lack of techniques to study the functions of these cells *in vitro*. An important advance was the development of an astrocyte culture preparation from rodent neonatal brains (McCarthy and de Vellis, 1980). Nearly all studies of astrocyte function since then have exploited this culture preparation. In this paper,

[*]Correspondence: lfoo@stanford.edu.

[1]Accession record number : GSE26066

astrocytes prepared using this method will be referred to as MD-astrocytes. Much has been learned about neuron-glial interactions from this method, but there are several limitations to its use. First, it is not prospective and isolation of astrocytes involves many steps extending over a week or more. Prospective isolation refers to the direct selection and isolation of a specific cell, without indirect steps extending over days or weeks. Second, while adult astrocytes *in vivo* exhibit limited division (Haas et al, 1970; Skoff and Knapp, 1991) and are highly process-bearing, MD-astrocytes divide rapidly and continuously; being able to be passaged for many months, and lack processes, being flat and fibroblast-like in morphology. Third, MD-astrocytes can only be prepared from neonatal brains at a time when their generation is just beginning. Few viable astrocytes can be obtained from postnatal or adult brain suspensions, when mature astrocytes are present *in vivo*. Fourth, it has recently been shown that MD-astrocytes have a gene expression profile that differs significantly from acutely isolated postnatal day 7 (P7) and P16 astrocytes (Cahoy et al., 2008) and adult *in vivo* astrocytes (Doyle et al, 2008). In addition, MD-astrocytes must be obtained by culture in an undefined, serum-containing media. This is highly non-physiological, as most serum proteins are unable to cross the blood-brain barrier and likely profoundly alter astrocyte properties (see discussion).

In this paper, we describe a new immunopanning method for prospectively isolating astrocytes from rodent CNS tissue. We have successfully isolated astrocytes from P1–P18 rats. Unlike the previous McCarthy and de Vellis method of astrocyte preparation, where cells were prepared by a series of steps extending over a week, we selected the astrocytes directly in a rapid isolation procedure that was completed in one day. We also report the development of a defined, serum-free medium that enables the survival of the purified astrocytes in long-term culture. Compared to MD-astrocytes, these immunopanned astrocytes, which we refer to in this paper as IP-astrocytes, maintain gene profiles in culture that much more closely mimic their acutely purified state. Lastly using this new IP-astrocytes preparation, we begin to unravel some of the fundamental functional properties of astrocytes.

Results

Purification of astrocytes from the postnatal rat cortex

We applied immunopanning techniques we have previously used to purify other major cell types of the central nervous system (CNS) (Barres et al., 1988, 1992) to isolate astrocytes. Due to the lack of known astrocyte-specific surface antigens, immunopanning of astrocytes has previously been impossible. We used the gene profiling data from Cahoy et al 2008 to select candidates expressed by astrocytes, then picked candidates for which specific monoclonal antibodies directed against surface epitopes, such as EGFR, FGFR3 and CD9, were available. We identified integrin beta 5 *(itgb5)* as highly expressed and an astrocyte-specific gene suitable for immunopanning. *Itgb5* is expressed highly in acutely purified mouse astrocytes both postnatally and in adult brain and was successful at purifying astrocytes from CNS rat cortex. Yield obtained after P14 fell rapidly because of the difficulty of extracting astrocytes viably (data not shown). This was not a significant limitation as astrocytes reach their plateau number between postnatal day 7 and 10 in rodent brain, a time by which their gene expression profiles are nearly indistinguishable from their adult gene profiles, providing evidence that the gene profiles of acutely isolated astrocytes very closely resemble *in vivo* cortical astrocyte gene profiles (Doyle et al., 2008).

We used a succession of negative immunopanning plates to remove other cell types from the dissociated cortical suspension including microglia, macrophages, endothelial cells, and oligodendrocyte precursor cells (OPCs) (Figure 1A). We then used a final panning plate coated with the ITGB5 monoclonal antibody to select for astrocytes. We validated the purity

of IP-astrocytes with RT-PCR against a battery of cell type-specific markers such as Bruno-like 4 (*Brunol4*) for neurons (identified to be highly neuron-specific, Cahoy et al, 2008), chemokine (C-X3-C motif) receptor (*CX3CR1*) for microglia and occludin for endothelial cells (Figure 1B). Before purification, the cortical suspension contained 25.1% GFAP+ cells, 24.9% microglia and endothelial cells, 8.4% oligodendrocytes, 31.7% neurons and 6.6% OPCs or pericytes as determined by immunostaining single cell cortical suspensions (data not shown). After isolation, 98.7% of the cells were GFAP+, indicating the high degree of purity of the IP-astrocytes (Figure 1B,C).

To assess if all or just a subset of IP-astrocytes express ITGB5, we immunostained cortical suspensions with ITGB5 and GFAP antibodies and quantified the number of GFAP+ cells that were also ITGB5+. 95.2±6.2% of GFAP+ cells were also ITGB5+, indicating that we have the ability to isolate the majority of the GFAP-expressing cells from the rat cortex (Figure 1D). The yield of purified astrocytes at P7 was approximately 10% of all cortical cells and 50% of all astrocytes in the starting suspension.

Identification of HBEGF as a trophic factor for astrocytes in vitro

Plating of IP-astrocytes P7 in serum-free media without any growth factors led to death of the majority of astrocytes by apoptosis within 40 hours as verified by staining with Annexin V, a marker of apoptosis (Figure 1E).

We thus sought to identify the trophic factor(s) that IP-astrocytes require for survival *in vitro* with the aid of our gene profiling data set. We generated a list of receptors expressed on the surface of astrocytes and cross-referenced this list with growth factors expressed by the major cell types in the brain and generated a list of candidates to test (Cahoy et al., 2008; Daneman et al., 2010).

We plated IP-astrocytes from P7 rats (IP-astrocytes P7) at a low density in a defined, serum-free base media with 0.5μg/ml of aphidicolin to inhibit cell division and assessed the ability of individual growth factors to promote the survival of astrocytes after 2 days *in vitro* (DIV). As 13% of astrocytes divided every 2 days (Figure S1A, see below), aphidicolin, an inhibitor of the cell cycle, was used to enable accurate determination of survival independently of division (Hughes and Cook, 1996). Aphidicolin itself did not significantly affect the survival of astrocytes (Figure S1B).

We tested many candidates from the list of cognate ligands for astrocyte receptors. However, these ligands did not confer significant, reliable or robust survivability. Among those tested were ciliary neurotrophic factor (CNTF) and thyroid hormone (T3) (Figure 2A), oncostatin M, sonic hedgehog, fibroblast growth factor 9 (FGF9), interleukin-11 (IL-11), brain-derived neurotrophic factor (BDNF), pleiotrophin, Wnt3a, Wnt5a, platelet-derived trophic factor BB, transforming growth factor β1 and 2 (data not shown).

We found that 5ng/ml of heparin-binding epidermal growth factor (HBEGF) was effective at keeping astrocytes alive compared to base conditions. HBEGF was very potent and consistently able to promote survival of astrocytes in serum-free culture (41.1±3.2% astrocytes survived, $p<0.001$, Figure 2A, S1F) for as long as 2 weeks and the cells extended multiple processes (Figure 1G). HBEGF promoted the survival of about 40–60% of the isolated IP-astrocytes. HBEGF is a member of the epidermal growth factor (EGF) family of growth factors (Citri and Yarden, 2006). As such, we also tested the survival-promoting ability of other EGF family members. 10ng/ml of transforming growth factor alpha (TGFα (41.6±4.5% astrocytes survived, $p<0.001$, Figure 2A) was as effective as HBEGF, but this was not additive (data not shown). Amphiregulin, however, was ineffective (Figure S1C).

HBEGF is a ligand for EGFR, erbB3 and erbB4 (Citri and Yarden, 2006). Acutely purified mouse IP-astrocytes express *egfr* and *erbb2* (Cahoy et al., 2008). ErbB2 is not believed to bind to any ligands but functions as a preferred heterodimeric co-receptor for other erbB receptors (Klapper et al., 1999; Citri and Yarden, 2006). We verified that acutely isolated mouse and rat IP-astrocytes express EGFR by Western blotting (Figure 2G). With immunostaining, we found that 92.6±2.4% of eGFP+ cortical astrocytes at P6 in brain sections were EGFR+, suggesting that they are receptive to HBEGF signaling (Figure 3A). We used a specific EGFR tyrosine kinase inhibitor, AG1478, to test if EGFR was the receptor mediating survival *in vitro* (Gan et al., 2007). Concentrations of 10μM and 30μM was sufficient to negate the effect of HBEGF, providing further evidence that EGFR is the signaling receptor for HBEGF that promotes the survival of astrocytes *in vitro*. AG1478 itself was not detrimental to baseline cell survival (Figure 2B).

We also found that Wnt7a at 1μg/ml was effective at promoting astrocyte survival (35.9±3.7% astrocytes survived, $p<0.05$) but the effect was not additive with HBEGF (37.0±2.8% astrocytes survived, Figure 2C). As the effect of HBEGF was robust and reliable, we focused the rest of the work in this paper on HBEGF.

Vascular cells promote IP-astrocyte P7 survival in vitro

To see if astrocytes themselves could secrete signals that promote their own survival, we assessed IP-astrocyte P7 survival with an IP-astrocyte P7 feeder layer. We found that IP-astrocytes P7 produced a soluble autocrine trophic factor that could keep other astrocytes alive (48.1%±0.8% astrocytes survived, $p<0.001$). This factor acted via EGFR as the effect was significantly reduced by addition of AG1478 (23.0%±2.4% astrocytes survived, $p<0.001$) (Figure 2D). In line with this result, when IP-astrocytes were plated at high densities either in inserts or on coverslips, they produced enough trophic factors to keep other astrocytes alive (Figure 2E, S1E).

Astrocytes have endfeet that make contact with blood vessels and thus contact both endothelial cells and pericytes. To test if vascular cells promoted astrocyte survival, we used feeder layers of endothelial cells, pericytes and a combination of pericytes and endothelial cells to assess if these cells secreted a factor that kept IP-astrocytes P7 alive. Pericytes significantly promoted IP-astrocyte P7 survival (46.8±4.3% astrocytes survived, $p<0.001$, Figure 2D, S1D,M) but this effect was insensitive to AG1478 (36.8±7.3% astrocytes survived, $p<0.05$, Figure 2D). Endothelial cells were effective at keeping IP-astrocytes P7 alive (49.0±2.5% astrocytes survived, $p<0.001$, Figure 2D, S1D,N) and this effect was significantly reduced with AG1478 (30.9±2.8% astrocytes survived, $p<0.001$, Figure 2D). The combination of pericytes and endothelial cells (33.2±7.1% astrocytes survived, $p<0.001$) had the highest percentage of astrocytes bearing 4 or more processes (Figure S1G, K–P) but did not confer more survivability than endothelial cells (33.7±5.5% astrocyte survived) or pericytes (42.9±4.3% astrocytes survived) alone (Figure S1D). Endothelial cells and astrocytes both express *hbegf* mRNA (Cahoy et al 2008, Daneman et al 2010). Our results suggest that the predominant factor produced by these two cell types is likely to be HBEGF acting via EGFR, but pericytes produce an unidentified trophic factor(s) that confers survivability via a distinct signaling pathway. Consistent with this, we found that endothelial cell conditioned media (ECM) and IP-astrocyte P1 conditioned media (P1 ACM) contained high levels of HBEGF, but IP-astrocytes P7 conditioned media (P7 ACM, Figure 2H, high exposure) contained low levels and pericyte conditioned media (PCM) did not contain HBEGF (Figure 2H). Depletion of P7 ACM with goat anti-HBEGF IgG negated the survival-promoting effect of P7 ACM, whereas P7 ACM treated with an irrelevant control antibody, goat anti-Gγ13 IgG, retained full survival-promoting activity (Figure 2F).

As we have demonstrated that vascular cells strongly promoted astrocyte survival *in vitro*, we next asked whether survival of astrocytes *in vivo* might be dependent upon vascular contact. We used two methods to investigate if every astrocyte directly contacted blood vessels. In the hippocampus, we injected DiI into blood vessels to delineate the vessels (or used DIC optics) and used patch-clamping to dye-fill astrocytes in 100μm slices of P14 and adult rats. We found that 100% of dye-filled astrocytes in both P14 (n=23) and adult rats (n=22) had endfeet that contacted blood vessels. At P14, astrocytes often extended long thin processes with an endfoot that contacted the blood vessel. Full ensheathement is completed by adulthood (Figure 3B,C). We also used an unbiased approach to sparsely label astrocytes in the cortex using mosaic analysis of double markers (MADM) in mice (Zong et al., 2005). hGFAP-Cre was used to drive inter-chromosomal recombination in cells with MADM-targeted chromosomes. We imaged 31 astrocytes in 100μm sections and co-stained with BSL-1 to label blood vessels and found that 30 astrocytes contacted blood vessels at P14 (Figure 3D,E). Together, we conclude that after the bulk of astrocytes have been generated, the majority of astrocytes contact blood vessels.

We hypothesized that if astrocytes are matched to blood vessels for survival during development, astrocytes that are over-generated and fail to establish a contact with endothelial cells may undergo apoptosis because of failure to obtain needed trophic support. By examining cryosections of developing postnatal brains from Aldh1L1-eGFP GENSAT mice, in which most or all astrocytes express green fluorescent protein (Cahoy et al 2008), immunostaining with the apoptotic marker activated caspase 3 and visualizing condensed nuclei, we found that the number of apoptotic astrocytes observed *in vivo* peaked at P6 and sharply decreased with age thereafter (Fig 3F,G). Death of astrocytes shortly after their generation and the elevated expression of *hbegf* mRNA in endothelial cells compared to astrocytes (Cahoy et al 2008, Daneman et al 2010) supports the hypothesis that astrocytes may require vascular cell-derived trophic support.

IP-astrocytes P7 divide more slowly compared to MD-astrocytes

MD-astrocytes show remarkable proliferative ability and can be passaged repeatedly over many months. In contrast, most astrocyte proliferation *in vivo* is largely complete by P14 (Skoff and Knapp, 1991). To directly compare the proliferative capacities of MD and IP-astrocytes P7, we plated dissociated single cells at low density in a defined, serum-free media containing HBEGF and counted clones at 1, 3 and 7DIV (Figure S1Q–S). MD-astrocytes displayed a much higher proliferative capacity, 75% of them dividing once every 1.4 days by 7DIV. In contrast, 71% of IP-astrocytes divided less than once every 3 days (Figure S1S). Thus IP-astrocytes have a more modest ability to divide compared with MD-astrocytes, this is more in line with what is expected *in vivo* (Skoff and Knapp 1991).

Gene expression of IP-astrocytes is closer to that of cortical astrocytes in vivo than MD-astrocytes

Using gene profiling, we determined if gene expression of cultured IP-astrocytes was more similar to that of acutely purified astrocytes, compared to MD-astrocytes. Total RNA was isolated from acutely purified astrocytes from P1 and P7 rat brains (IP-astrocytes P1 and P7) and from acutely isolated cells cultured for 7DIV with HBEGF (IP-astrocytes P1 and P7 7DIV respectively) and from MD-astrocytes (McCarthy and de Vellis, 1980).

RT-PCR with cell-type specific primers was used to assess the purity of the isolated RNA. We used *GFAP*, *brunol4*, *MBP*, occludin, *CX3CR1* as mentioned above, as well as chondroitin proteoglycan sulfate 4 (*CSPG4*) for OPCs and pericytes. MD-astrocytes consistently had some neuron contamination because of the high percentage of

contaminating neural stem cells (Hildebrand et al, 1997) (Figure 4A). This was not observed in IP-astrocyte cultures.

IP-Astrocytes P1 and P7 7DIV cells had an expression profile resembling their acutely isolated counterparts, where only 118 and 54 genes respectively differed significantly ($p<0.05$). In contrast, MD-astrocyte expression profiles were significantly different from that of acutely purified cells (Table 1, Figure 4B). With a very stringent statistical test (moderated t-test) and post test (Bonferroni correction) to identify the most significant changes, we found that 547 and 729 genes were significantly different ($p<0.05$) between acute IP-astrocytes P1 or P7 cells and MD-astrocytes respectively. These results strongly suggest that by gene expression, cultured IP-astrocytes are more similar to cortical astrocytes *in vivo*.

Only 54 genes out of over 31,000 genes differed significantly between acute IP-astrocytes P7 and IP-astrocytes P7 7DIV ($p<0.05$). Of these, 51 genes were higher in acute cells than in culture (Table 1). This is unsurprising as in culture, many signals and cell-cell interactions are missing hence, many signaling pathways would be turned off in the absence of the initiating ligands. We generated tables of the top 30 genes that differed significantly ($p<0.05$) and ≥8-fold different between cultured IP-astrocytes and their acutely isolated counterparts (Table S1 and S2). As several genes were turned off in both cultured IP-astrocytes P1 and P7 cells, there is likely a common signal in the brain regulating the expression of these genes at both ages that is absent in the defined serum-free culture media.

To understand the significance of the differentially expressed genes, we used Ingenuity Pathway Analysis (IPA) to generate lists of pathways that are activated in acutely isolated astrocytes but are off in the cultured cells. Two pathways that were turned off in P7 astrocytes upon culture were the Wnt and Notch pathways (Table S3).

We also found that many genes involved in modulating the cell cycle such as *ccnb1*, *cdkn1a* and *ccnd1* were much higher in MD-astrocytes versus cultured IP-astrocytes P7. Canonical pathways significantly higher in MD-astrocytes compared to IP-astrocytes were those involved in G2/M DNA damage, cyclins and cell cycle regulation and G1/S checkpoint regulation ($p<0.05$). In contrast, no pathways involved in cell cycle regulation were higher in cultured IP-astrocytes P7 compared to MD-astrocytes. This pathway analysis result is in line with what we observe with regards to the higher proliferative capacity of MD-astrocytes.

Understanding the effect of serum on astrocytes

Unlike IP-astrocytes that are cultured in serum-free media, MD-astrocytes must be cultured in serum right after isolation, hence the gene expression differences could be caused by serum exposure. To address this question and to elucidate the genes induced by serum in IP-astrocytes, we cultured IP-astrocytes right after isolation in MD-astrocyte growth media for 7 days (10% serum). At 7 days, total RNA was either collected (IP-astrocytes P7 7DIV serum) or the serum replaced with base media containing HBEGF for an additional 7 days before collecting the RNA for gene profiling analysis (IP-astros P7 14DIV withdraw).

365 genes were induced in the IP-astrocytes by serum (Figure 4C), however few of these corresponded to genes expressed by the MD-astrocytes. Of the top 30 genes induced by serum in IP-astrocytes, 8 of 30 genes were expressed highly (>1000) in MD-astrocytes and 8 of 30 were moderately expressed (>200 but <1000) (Table 2). The other 14 genes induced by serum in IP-astrocytes P7 were not expressed by MD-astrocytes. In addition, the serum induced genes did not revert back to the levels observed in IP-astrocytes P7 7DIV. 302 of the 365 serum-induced genes continued to be expressed after serum withdrawal.

Additionally, of the pathways in IP-astrocytes P7 7DIV significantly induced by serum ($p<0.05$), 16 of 28 remained active after serum withdrawal (Table S4,5).

Together our data shows that differences between MD-astrocytes and IP-astrocytes cannot be explained by serum exposure alone and that serum exposure causes lasting gene expression changes that persist after serum withdrawal.

Confirming functional properties of astrocytes in culture

The much closer match of cultured IP-astrocyte gene profiles to those of acutely purified astrocytes indicates that IP-astrocyte cultures are better models of astrocytes than are MD-astrocytes. We therefore assessed whether IP-astrocytes exhibited well-characterized astrocytic functions in culture.

MD-astrocytes promote CNS neuron survival in culture (Banker 1980, Wagner et al 2006). We asked if the cultured IP-astrocytes could similarly promote CNS neuronal survival. We purified P5 retinal ganglion cells (RGCs) by immunopanning as described in Barres et al 1998 and added conditioned media (CM) from P1 (IP-astrocytes P1 ACM) or P7 astrocytes (IP-astrocytes P7 ACM). RGC growth media (RGC GM) and MD-astrocytes CM (MD-ACM) were used as positive controls. In the absence of any growth factors or astrocyte-derived media, fewer than 5% of RGCs survive. Both P1 ACM and P7 ACM (*$p<0.05$, **$p<0.01$), were as strongly effective at promoting RGC survival for 3 days in culture as was MD-ACM (Figure 5A,B).

Astrocytes are known to secrete many proteins that have been shown to be important in the CNS for instance apolipoprotein E (APOE), amyloid precursor protein (APP) and thrombospondin 2 (TSP2) (Farber et al., 1995; Mauch et al., 2001; Christopherson et al., 2005). We verified with Western blotting that ACM from MD-astrocytes, IP-astros P1 and P7 contained these three proteins. A Coomassie stain was used to verify that equivalent amounts of protein was loaded (Figure 5C). Both P1 ACM and P7 ACM contained APOE and APP. However, only P7 ACM contained TSP2. This differential protein expression at different astrocyte ages shows that we can use this new culture system to tease apart the roles of astrocytes at different developmental time points based on our ability to purify astrocytes at different ages. Interestingly, MD-ACM contained much higher levels of APP, TSP2 and APOE, molecules known to be critical regulators of synapse formation and function (Figure 5D–F). These results questioned whether IP-astrocytes were as capable as MD-astrocytes at inducing the formation of structural and functional synapses in culture.

To directly address this question, we next tested the ability of IP-astrocytes to induce structural synapses by exposing RGCs to feeder layers of P1, P7 IP-astrocytes, MD-astrocytes or a control with no astrocytes. Neuronal cultures were stained for bassoon, a pre-synaptic marker and homer, a post-synaptic marker (Figure 5G). The number of co-localized puncta in each condition were quantified and we have plotted the number of co-localized puncta as a fold change over control (Figure 5H). There were significant increases in synapse number over control with MD-astrocytes (fold change=3.12, $p<0.01$), P1 (fold change=2.57, $p<0.05$) and P7 (fold change=2.86, $p<0.01$) IP-astrocyte inserts, (Figure 5G–H). Thus, IP-astrocytes are as capable of inducing structural synapses in RGC cultures as MD astrocytes are.

Structural synapses are not indicative of functional synapses, thus we analyzed synaptic activity of the RGCs in the presence of a feeder layer of astrocytes. Previous studies have shown that the number of functional synapses increases significantly with an MD-astrocyte feeder layer (Ullian et al., 2001). We found that both the frequency and amplitude of miniature excitatory postsynaptic currents (mEPSCs) increased significantly and to a

comparable degree with feeder layers of IP-astrocytes P1 or P7, to that observed with an MD-astrocyte feeder layer (Figure 5I–L). Taken together, these results show that IP-astrocytes retain functional properties characteristic of astrocytes.

Calcium imaging of astrocytes

Intracellular calcium oscillations have been observed in astrocytes *in vivo* and are considered an important functional property of astrocytes and may aid in regulation of blood flow or neural activity (Nimmerjahn et al., 2009). Several stimuli have been implicated in initiating calcium waves in MD-astrocytes. We used calcium imaging with Fluo-4 to investigate if IP-astrocytes exhibit calcium rises in response to glutamate, adenosine, potassium chloride (KCl) and ATP and if the nature of their response was similar to MD astrocytes (Cornell-Bell et al., 1990; Jensen and Chiu, 1991; Kimelberg et al., 1997; Pilitsis and Kimelberg, 1998).

Few calcium oscillations were observed at rest in IP-astrocytes, contrary to MD-astrocytes. A single cell in confluent cultures of P7 IP-astrocytes would respond independently of its neighbors. Such isolated and spontaneous firing of astrocytes has previously been observed in brain slices (Nett et al., 2002; Parri and Crunelli, 2003). In contrast, rhythmic calcium activity and regular spontaneous activity were observed in MD-astrocytes grown in the same media as cultured IP-astrocytes P7 (Figure 6A,C).

Both MD-astrocytes and IP-astrocytes responded to 10μM of adenosine (100% of MD-astrocytes, 89.6±5.5% of IP-astrocytes, Figure S2C,D), 50μM of glutamate (100% of MD-astrocytes, 88.1±7.9% of IP-astrocytes, Figure S2E,F) and 100μM of ATP (94.4±5.5% of MD-astrocytes, 92.5±1.5% of IP-astrocytes, Figure 6A,B) with increased frequency of calcium oscillations and/or amplitude of calcium oscillations. Both have several P2X and P2Y receptors and *adora1* and *adora2b* receptors and thus can respond to these stimuli. Both MD and IP-astrocytes express mRNA for ionotropic glutamate receptors, but only the latter have metabotropic receptors[1]. Thus, the second phase calcium response observed with glutamate in IP-astrocytes after a period of quiescence, could be a metabotropic response. This was not observed in MD-astrocytes.

KCl has been reported to depolarize MD-astrocytes and induce vesicular release of gliotransmitters in a calcium-dependent manner (Paluzzi et al., 2007). We found that 50mM KCl caused more MD-astrocytes to respond (83.3±4.4%, n=275 cells, $p<0.0001$, Figure 6C). In contrast, IP-astrocytes consistently failed to respond to KCl (0.3±0.2%, n=749 cells, Figure 6D). Control conditions yielded few responses in both MD-astrocytes (17.9±7.4% cells respond, n=118 cells) and IP-astrocytes (4.5±3.4% cells respond, n=95 cells, Figure S2A,B).

Immunostaining cultures after imaging with MBP, NG2 and TUJ1 revealed high numbers of contaminating oligodendrocytes, OPCs and neurons in MD-astrocyte cultures (Figure 6H–J) but not in IP-astrocyte cultures. To test if the response of MD-astrocytes was an indirect consequence of neuronal depolarization, we incubated MD-astrocyte cultures with 100nM bafilomycin-A1, an inhibitor of vacuolar-type ATPases, to block neurotransmitter release by neurons (Zhou et al., 2000; Nett et al., 2002). This did not eliminate MD-astrocyte responses as 83.3±5.1% of the cells still responded (n=558), alter the level of neuronal contamination nor alter the response to 100μM ATP (Figure S2G–J). Interestingly, we found that growing

IP-astrocytes for 3 days in MD-astrocyte growth media (AGM) containing 10% serum significantly increased the percentage of IP-astrocytes (53.3±7.4%, $p<0.001$, n=209 cells, Figure 6F) responding to KCl, compared to control conditions of IP-astrocytes grown in AGM (18.9±5.7%, n=134 cells, Figure 6E). We found no increase in contaminating cell types in serum-treated IP-astrocytes cultures (data not shown). These findings suggest that serum exposure alters the properties and functions of astrocytes in culture and that IP-astrocytes, based on their expression profiles and physiology, are more representative of *in vivo* astrocytes.

Astrocytes do not release glutamate in culture in response to ATP

Astrocytes have been reported to release glutamate both *in vitro* and *in vivo* in response to stimuli such as ATP that elevate their intracellular levels of calcium (Parpura et al 1994, Pasti et al 1997, Hamilton and Attwell 2010). To investigate if IP-astrocytes exhibit regulated release of glutamate, we used the sensitive method of HPLC with tandem mass spectrometry analysis, to detect glutamate in cultures of IP and MD-astrocytes in response to 100μM of ATP. As a positive control, we stimulated cultures of RGCs with KCl and readily detected glutamate (1880nM) in the media after 5mins of stimulation ($p<0.001$ over unstimulated neurons). However, glutamate was not detected in both IP- and MD-astrocytes cultured in HBEGF or AGM in response to ATP (Figure 6G). Control experiments where we loaded IP or MD-astrocytes for 5mins with 0.5μM of glutamate prior to stimulation did not lead to regulated release of glutamate by IP or MD-astrocytes (data not shown). Our results demonstrate that under these conditions, ATP does not induce glutamate release by astrocytes.

Discussion

We have developed a technique that allows prospective purification of astrocytes from the postnatal rat cortex, established serum-free conditions that promote their survival *in vitro*, and shown that their expression profiles in these cultures more closely resemble that of cortical astrocytes *in vivo* than the traditional McCarthy-de Vellis preparation of cultured neonatal astrocytes.

Astrocytes can be prospectively purified from CNS cell suspensions

Cell purification provides a powerful method that enables the study of the intrinsic properties of a cell type and its interactions with other cell types. Despite their abundance in the CNS, study of astrocytes has been hindered by the lack of a method for their prospective purification. The McCarthy and de Vellis method (1980) has been an invaluable method for isolation of neonatal astrocyte-like cells, but it has been unclear if these cells are good models of astrocytes *in vivo* as their isolation was not prospective and involved passage in serum containing medium. As these MD-astrocytes can only be obtained from neonatal brain, it has been speculated that these cells may be more akin to radial glia, astrocyte progenitor cells or reactive astrocytes. Indeed our recent gene profiling studies demonstrated that MD-astrocytes highly express hundreds of genes that are not normally expressed *in vivo* (Cahoy et al, 2008) and in more recent work we have found that their profiles indicate that they may be a combination of reactive and developing astrocytes (J. Zamanian, LCF, BAB, in preparation).

Prospective purification is important as it ensures that the selected astrocytes are representative of the whole population, avoiding the selection of a minor subset. In the MD-astrocyte preparation procedure, only a small percentage of astrocyte-like cells in the starting neonatal suspension survive in culture (our unpublished observations). Prospective purification also avoids prolonged culture of the cells in serum, which can irreversibly alter

the properties of the cells. By combining a series of depletion panning steps to remove unwanted cell types such as microglia followed by a selection step using a monoclonal antibody to integrin beta 5, we have been able to prospectively isolate differentiated astrocytes from P1 to P18 rat brain tissue at a purity of 99% and a yield of 50% of all astrocytes at P7. Although we have focused on the isolation of rat astrocytes in this work, we have developed a similar panning method to purify astrocytes to greater than 95% purity from postnatal mouse brain (Methods and Materials). This will enable astrocyte isolation from mutant or diseased mice, further facilitating the understanding of the functional role of astrocytes. Theoretically, this method can be extended to the purification of human astrocytes by using an appropriate ITGB5 antibody.

Astrocytes require trophic factors for survival

It has long been thought that astrocytes, unlike other brain cell types, may not need trophic signals to survive. Astrocytic cell death was reported in the postnatal rat cerebellum (Soriano et al., 1993; Krueger et al., 1995), however as astrocytes are phagocytic cells (al-Ali and al-Hussain, 1996) the presence of apoptotic nuclei within astrocytes could be phagocytozed apoptotic neurons. We have observed that majority of prospectively isolated CNS astrocytes (IP-astrocytes) die within 40 hours by apoptosis when cultured without any trophic factors and identified HBEGF and Wnt7a as effective at promoting significant astrocyte survival *in vitro*. Previous studies have underlined the necessity of EGFR for survival in the cortex, however, the relevant ligand for EGFR has not been identified (Kornblum et al 1999; Wagner et al., 2006). Our finding that HBEGF strongly promotes astrocyte survival *in vitro*, together with its high level in vascular cells (Daneman et al., 2010) strongly suggests that HBEGF is an excellent candidate for the ligand mediating astrocyte survival *in vivo*.

Do developing astrocytes compete for a limiting amount of endogenous trophic factor as do developing neurons and oligodendrocytes, which are matched to a limited number of target cells and axons respectively (Barres et al., 1992)? Indeed, we have observed astrocytic apoptosis during the peak of astrogenesis *in vivo*. As we found that HBEGF is highly expressed by developing vascular cells, that vascular cells help promote astrocyte survival, and that the majority of the astrocytes we analyzed contacted blood vessels, we hypothesize that a similar matching may occur between astrocytes and blood vessels. Excess, un-needed astrocytes generated where blood vessels are already ensheathed by other astrocytes may undergo elimination by apoptosis. This hypothesis can be tested in future experiments by assessing whether astrocytes fail to survive in adult mice in which blood vessels are eliminated by exposure to hyperoxia (Ndubuizu et al 2010).

Differentiated astrocytes have only a modest ability to divide

It is generally thought that differentiated astrocytes retain a high ability to proliferate. This hypothesis is based on the existence of highly proliferative glial CNS tumors and as astrocytes in MD-astrocyte cultures are so highly proliferative. However, we show that prospectively purified postnatal astrocytes cultured in HBEGF, a mitogenic signal, display only a modest ability to proliferate, dividing once every three days, whilst MD-astrocytes divide every 1.4 days. Even after astrocytes had reached their plateau numbers in the CNS by about P14 (Skoff and Knapp 1991), we found that they still retained this modest ability to divide (data not shown). Thus, most cortical astrocytes are not terminally postmitotic, but have a modest ability to divide (Skoff and Knapp, 1991), in keeping with recent findings on the limited proliferation of reactive astrocytes after brain injury (J. Zamanian, LCF, BAB, in preparation).

Prospectively purified immunopanned astrocyte cultures as a new preparation for understanding astrocyte function

The function of astrocytes has long been an intriguing mystery. As neurons depend on astrocytes for their survival, it has not been possible to get at their functional roles *in vivo* simply by deleting them. Culture studies thus provide a powerful approach. While MD-astrocytes have been a useful model system, we have shown here they are not optimal models of *in vivo* differentiated, more mature astrocytes. Therefore in this report, we have studied the functions of the more mature IP-astrocytes by co-culturing them with CNS neurons. We found that these astrocytes strongly stimulated neuronal survival and formation of functional synapses just as do the MD-astrocytes. In other cases however we observed differences in the behavior of the MD- and IP- astrocytes.

For instance there are differing responses of MD-astrocytes and IP-astrocytes to various stimuli such as glutamate and KCl and we speculate that this could be due to serum exposure and/or contaminating cells. In fact, we often observed spontaneous calcium activity in the absence of a stimulus in MD but not IP-astrocytes. Similar calcium activity in astrocytes has been observed in slices and has been shown to be dependent on neuronal activity (Aguado et al., 2002; Kuga et al., 2011), providing further evidence that observations made in cultures of MD-astrocytes could be due to neuronal contamination. The marked difference between the response of MD-astrocytes and IP-astrocytes to KCl stimulation is striking. A robust response is observed in MD-astrocytes but not IP-astrocyte cultures, unless they were exposed to serum. Interestingly, astrocytes in brain slices lacked a calcium response to KCl application, but responded to neuronal depolarization by KCl application due to neuronal glutamate release after a delay of several seconds (Pasti et al., 1997). Thus, IP-astrocyte cultures have a KCl response that is more representative of *in vivo* astrocytes, further validating this new astrocyte preparation.

We therefore used IP-astrocyte cultures to investigate the currently controversial issue of whether astrocytes are capable of induced glutamate release. Several reports have suggested that, rather than degrading glutamate, astrocytes *in vitro* and *in vivo* can accumulate, store, and release glutamate in a regulated manner (Hamilton and Attwell 2010). However, while we could easily detect glutamate release from neurons, neither MD- nor IP-astrocytes released detectable amounts of glutamate when stimulated with ATP. We speculate that previous reports that MD-astrocytes secrete glutamate in culture could be due to variable levels of contaminating cells in these cultures.

As IP-astrocytes are cultured in a defined media, without serum, and have gene profiles that closely resemble cortical astrocytes *in vivo*, these cultures promise to be very useful in understanding the fundamental properties of astrocytes. Many interesting questions can now be studied. For instance, what are the effects of stimulation of astrocytes with ligands of their various highly expressed transmembrane receptors? What transcriptional changes occur in astrocytes following sustained increase in intracellular calcium levels during repetitive neuronal stimulation? What are the interactions of astrocytes with other cell types such as neurons and endothelial cells? What are the signals that induce astrocytes to become reactive glial cells, is gliosis a reversible phenotype, and what are the functions of reactive astrocytes? Also, the ability to culture purified astrocytes will enable a metabolomics comparison of the signals secreted by astrocytes, neurons, and oligodendrocytes, enabling novel neuron-glial signals to be identified. Importantly, our methods can be simply modified to isolate human astrocytes to compare the functional properties of rodent and human astrocytes directly. This will enable comparison of their ability to induce synapse formation and function and elucidation of the signals responsible, both in health and disease.

Experimental Procedures

For detailed procedures, including detailed rodent panning protocol, see supplemental materials.

Tissue dissociation

6–10 postnatal Sprague Dawley rat cortices were enzymatically then mechanically dissociated to produce single cells before passing over successive negative panning plate to rid the cell suspension of microglia, endothelial cells, OPCs before selecting for astrocytes with an ITGB5-coated plate.

Survival Assay and culture conditions of immunopanned astrocytes

For all survival studies, IP-astrocytes were cultured at 2,500 cells/coverslip in a 24-well plate in a minimal media (see supplemental methods) with 0.5μg/ml aphidicolin (Sigma A0781). Individual growth factors were added to base media for testing. Survival was assayed 40h after plating using the Live/Dead Kit (Invitrogen L3224). 3 coverslips counted per condition. Used 1-way ANOVA with Bonferonni correction for statistics. Error bars represent SEM.

Inserts of astrocytes, endothelial cells and/or pericytes were used to condition base media for 1 day before addition to freshly isolated IP-astrocytes to assess survival.

Immunopanning with mouse astrocytes

We added 100μl of 0.5mg/ml sheep anti-ITGB5 (R&D Systems, AF3824) into 5–10ml of cell suspension after negative panning steps and incubated the cells for 30–40mins at 24°C. 3ml of 100% FCS/10ml media was added and the cells spun at 1000rpm for 10min. The supernatant was discarded and the cell pellet resuspended in 0.02% BSA and plated onto an anti-sheep IgG-coated petri dish.

Dye-filling of astrocytes

Hippocampal astrocytes from P14 and adult rat were located in 100μm thick sections by IR-DIC and iontophoretically filled with 5% aq. Lucifer yellow. Vessels were visualized with DIC (P14) or transcardial perfusion of DiI (adult). The slices were imaged on an Olympus FV1000 using a 60X oil objective (NA 1.40). Confocal volumes were analyzed and rendered using Imaris (Bitplane).

Immunostaining of brain sections

10μm thick sagittal cryosections were immunostained with EGFR (Millipore #06-847) or activated caspase 3 (BD Pharmingen 559565) overnight at 4°C. Images were taken at 40x on a Zeiss Axiocam microscope.

100μm MADM brain sections were stained with anti-GFP (1:1000, Abcam AB13970) and BSL-I (1:100, Vector labs, B-1105) for 3 days at 4°C. Secondary antibodies were incubated at 4°C, overnight. Images made with a 63x Plan Apochromat oil objective on a LSM 510 Meta Confocal scope.

Immunodepletion of ACM

P7 ACM was incubated overnight with anti-HBEGF (sc-1414) or goat anti-Gγ13 IgG (sc-26781) conjugated to Protein A/G beads then added to base media to assess survival. 3 biological replicates. 1-way ANOVA with Bonferroni correction method. Error bars represent SEM.

Sample preparation and gene expression analysis

Total RNA isolated with QIAshredder and Qiagen RNeasy Mini Kit. Used the 3'IVT Express kit for preparation of the RNA and the Rat Genome 230 2.0 Array chip (Affymetrix, Santa Clara). Expression values were generated for our datasets using the RMA method with the ArrayStar program from DNASTAR, Inc. All statistical analyses and clustering done with ArrayStar.

We filtered genes that had an expression value over 200 in any sample and performed unsupervised hierarchical clustering on these 15,960 genes. To calculate statistical values, we used a moderated t-test with the Bonferroni correction method.

Neuronal survival and synapse formation assays

15μg of protein from IP or MD-astrocyte CM was added to RGC minimal media. RGC growth media is RGC minimal media with 50ng/ml of BDNF (Peprotech 450-02), 10ng/ml CNTF, 50μg/ml insulin (Sigma I6634) and B27 supplement. RGCs were purified as previously described (Barres et al 1988) and plated at 15,000 cells/well and survival was assessed after 3 days (n=3).

RGCs were cultured for 7 days in RGC growth media and inserts of astrocytes added for 6 more days (n=3). After 6 days, cells were fixed for 10mins with 4% PFA and stained for Bassoon and Homer. Puncta Analyzer plugin was used to quantify synapses in ImageJ. 1-way ANOVA with Bonferonni correction was used to calculate statistics. Error bars represent SEM.

Electrophysiology

Miniature excitatory postsynaptic currents (mEPSCs) were recorded by whole-cell patch clamping RGCs at room temperature (18°C–22°C) at a holding potential of −70 mV. The extracellular solution contained 140 NaCl, 2.5 CaCl2, 2 MgCl2, 2.5 KCl, 10 glucose, 1 NaH_2PO_4 and 10 HEPES (pH 7.4) (in mM), plus TTX (1 μM) to isolate mEPSCs. Patch pipettes were 3–5 MΩ and the internal solution contained (in mM) 120 K-gluconate, 10 KCl, 10 EGTA, and 10 HEPES (pH 7.2). mEPSCs were recorded using pClamp software for Windows (Axon Instruments, Foster City, CA), and were analyzed using Mini Analysis Program (SynaptoSoft, Decatur, GA) (n=3).

Western blotting

Blots were probed with rabbit anti-human EGFR (Cell Signaling 2232), mouse antihuman actin (Abcam 8226), APOE, TSP2 and APP and rabbit anti-rat HBEGF antibody (kind gift from Prof F. Zeng) were used. Pierce GelCode Blue Stain reagent was used for coomassie staining.

Quantitation of Glutamate

Astrocytes were cultured in either base media containing 5ng/ml HBEGF or MD-astrocyte growth media (AGM) containing 10% FCS. RGCs were grown for 7d in RGC. Cells were washed with HEPES-Buffered Ringers' 3x before stimulation. 100μM of ATP was used for stimulation and 100μM of DL-TBOA used to block glutamate transporters. 200μl of Ringer's was added onto the cells and the cells incubated at 37°C for 5min. 150μl of media was collected after 5mins and sent to Brains On-Line, LLC for quantitation by mass spectrometry.

Access to gene expression data

Raw .CEL files for all samples used for gene expression analysis in the paper can be accessed via the NCBI Gene Expression Omnibus (GEO) database at http://www.ncbi.nlm.nih.gov/geo/query/acc.cgi?token=hrgdzmgcyiyuots&acc=GSE26066, Accession record number: GSE26066. 1.

Supplementary Material

Refer to Web version on PubMed Central for supplementary material.

Acknowledgments

We thank M. Fabian and A. Ibrahim for technical support, M van der Hart of Brains One-Line, LLC for the mass spectrometry analysis of the glutamate samples and Prof F. Zeng for the anti-rat HBEGF antibody. This work was supported by grants from NIH R01 NS059893 (B.A.B) and the Agency for Science, Technology and Research, Singapore (L.C.F). We thank Vincent and Stella Coates for their generous support.

Bibliography

1. Aguado F, Espinosa-Parrilla JF, Carmona MA, Soriano E. Neuronal Activity Regulates Correlated Network Properties of Spontaneous Calcium Transients in Astrocytes In Situ. J. Neurosci. 2002; 22:9430–9444. [PubMed: 12417668]
2. al-Ali SY, al-Hussain SM. An ultrastructural study of the phagocytic activity of astrocytes in adult rat brain. Journal of anatomy. 1996; 188(Pt 2):257–262. [PubMed: 8621323]
3. Banker GA. Trophic interactions between astroglial cells and hippocampal neurons in culture. Science. 1980; 209:809–810. [PubMed: 7403847]
4. Barres BA, Silverstein BE, Corey DP, Chun LL. Immunological, morphological, and electrophysiological variation among retinal ganglion cells purified by panning. Neuron. 1988; 1:791–803. [PubMed: 2908449]
5. Barres BA, Hart IK, Coles HS, Burne JF, Voyvodic JT, Richardson WD, Raff MC. Cell death and control of cell survival in the oligodendrocyte lineage. Cell. 1992; 70:31–46. [PubMed: 1623522]
6. Cahoy JD, Emery B, Kaushal A, Foo LC, Zamanian JL, Christopherson KS, Xing Y, Lubischer JL, Krieg PA, Krupenko SA, et al. A transcriptome database for astrocytes, neurons, and oligodendrocytes: a new resource for understanding brain development and function. J Neurosci. 2008; 28:264–278. [PubMed: 18171944]
7. Christopherson KS, Ullian EM, Stokes CCA, Mullowney CE, Hell JW, Agah A, Lawler J, Mosher DF, Bornstein P, Barres BA. Thrombospondins Are Astrocyte-Secreted Proteins that Promote CNS Synaptogenesis. Cell. 2005; 120:421–433. [PubMed: 15707899]
8. Citri A, Yarden Y. EGF-ERBB signalling: towards the systems level. Nat Rev Mol Cell Biol. 2006; 7:505–516. [PubMed: 16829981]
9. Cornell-Bell AH, Finkbeiner SM, Cooper MS, Smith SJ. Glutamate induces calcium waves in cultured astrocytes: long-range glial signaling. Science. 1990; 247:470–473. [PubMed: 1967852]
10. Daneman R, Zhou L, Agalliu D, Cahoy JD, Kaushal A, Barres BA. The Mouse Blood-Brain Barrier Transcriptome: A New Resource for Understanding the Development and Function of Brain Endothelial Cells. PLoS ONE. 2010; 5:e13741. [PubMed: 21060791]
11. Doyle JP, Dougherty JD, Heiman M, Schmidt EF, Stevens TR, Ma G, Bupp S, Shrestha P, Shah RD, Doughty ML, et al. Application of a translational profiling approach for the comparative analysis of CNS cell types. Cell. 2008; 135:749–762. [PubMed: 19013282]
12. Eroglu C, Barres BA. Regulation of synaptic connectivity by glia. Nature. 2010; 468:223–231. [PubMed: 21068831]
13. Farber SA, Nitsch RM, Schulz JG, Wurtman RJ. Regulated secretion of beta-amyloid precursor protein in rat brain. J Neurosci. 1995; 15:7442–7451. [PubMed: 7472496]
14. Gan HK, Walker F, Burgess AW, Rigopoulos A, Scott AM, Johns TG. The epidermal growth factor receptor (EGFR) tyrosine kinase inhibitor AG1478 increases the formation of inactive

untethered EGFR dimers. Implications for combination therapy with monoclonal antibody 806. J Biol Chem. 2007; 282:2840–2850. [PubMed: 17092939]

15. Haas RJ, Werner J, Fliedner TM. Cytokinetics of neonatal brain cell development in rats as studied by the 'complete 3H-thymidine labelling' method. Journal of anatomy. 1970; 107:421–437. [PubMed: 5492936]
16. Hamilton NB, Attwell D. Do astrocytes really exocytose neurotransmitters? Nature reviews. 2010; 11:227–238.
17. Hildebrand B, Olenik C, Meyer DK. Neurons are generated in confluent astroglial cultures of rat neonatal neocortex. Neuroscience. 1997; 78:957–966. [PubMed: 9174064]
18. Hughes TA, Cook PR. Mimosine Arrests the Cell Cycle after Cells Enter S-Phase. Experimental Cell Research. 1996; 222:275–280. [PubMed: 8598214]
19. Jensen AM, Chiu SY. Differential intracellular calcium responses to glutamate in type 1 and type 2 cultured brain astrocytes. J. Neurosci. 1991; 11:1674–1684. [PubMed: 1675265]
20. Kimelberg HK, Cai Z, Rastogi P, Charniga CJ, Goderie S, Dave V, Jalonen TO. Transmitter-induced calcium responses differ in astrocytes acutely isolated from rat brain and in culture. Journal of neurochemistry. 1997; 68:1088–1098. [PubMed: 9048754]
21. Klapper LN, Glathe S, Vaisman N, Hynes NE, Andrews GC, Sela M, Yarden Y. The ErbB-2/HER2 oncoprotein of human carcinomas may function solely as a shared coreceptor for multiple stroma-derived growth factors. Proceedings of the National Academy of Sciences of the United States of America. 1999; 96:4995–5000. [PubMed: 10220407]
22. Kornblum HI, Zurcher SD, Werb Z, Derynck R, Seroogy KB. Multiple trophic actions of heparin-binding epidermal growth factor (HB-EGF) in the central nervous system. The European journal of neuroscience. 1999; 11:3236–3246. [PubMed: 10510187]
23. Krueger BK, Burne JF, Raff MC. Evidence for large-scale astrocyte death in the developing cerebellum. J. Neurosci. 1995; 15:3366–3374. [PubMed: 7751916]
24. Kuga N, Sasaki T, Takahara Y, Matsuki N, Ikegaya Y. Large-Scale Calcium Waves Traveling through Astrocytic Networks In Vivo. J. Neurosci. 2011; 31:2607–2614. [PubMed: 21325528]
25. Mauch DH, Nagler K, Schumacher S, Goritz C, Muller E-C, Otto A, Pfrieger FW. CNS Synaptogenesis Promoted by Glia-Derived Cholesterol. Science. 2001; 294:1354–1357. [PubMed: 11701931]
26. McCarthy KD, de Vellis J. Preparation of separate astroglial and oligodendroglial cell cultures from rat cerebral tissue. J. Cell Biol. 1980; 85:890–902. [PubMed: 6248568]
27. Ndubuizu OI, Tsipis CP, Li A, LaManna JC. Hypoxia-inducible factor-1 (HIF-1)-independent microvascular angiogenesis in the aged rat brain. Brain Research. 2010; 1366:101–109. [PubMed: 20875806]
28. Nedergaard M, Ransom B, Goldman SA. New roles for astrocytes: redefining the functional architecture of the brain. Trends Neurosci. 2003; 26:523–530. [PubMed: 14522144]
29. Nett WJ, Oloff SH, McCarthy KD. Hippocampal Astrocytes In Situ Exhibit Calcium Oscillations That Occur Independent of Neuronal Activity. Journal of neurophysiology. 2002; 87:528–537. [PubMed: 11784768]
30. Nimmerjahn A, Mukamel EA, Schnitzer MJ. Motor Behavior Activates Bergmann Glial Networks. 2009; 62:400–412.
31. Paluzzi S, Susanna A, Simona Z, Marco M, Luca R, Mario N, Giambattista B. Adult astroglia is competent for Na^{+}/Ca2+ exchanger-operated exocytotic glutamate release triggered by mild depolarization. Journal of neurochemistry. 2007; 103:1196–1207. [PubMed: 17935604]
32. Parpura V, Basarsky TA, Liu F, Jeftinija K, Jeftinija S, Haydon PG. Glutamate-mediated astrocyte-neuron signalling. Nature. 1994; 369:744–747. [PubMed: 7911978]
33. Parri HR, Crunelli V. The role of Ca2+ in the generation of spontaneous astrocytic Ca^{2+} oscillations. Neuroscience. 2003; 120:979–992. [PubMed: 12927204]
34. Pasti L, Volterra A, Pozzan T, Carmignoto G. Intracellular Calcium Oscillations in Astrocytes: A Highly Plastic, Bidirectional Form of Communication between Neurons and Astrocytes In Situ. J. Neurosci. 1997; 17:7817–7830. [PubMed: 9315902]
35. Pilitsis JG, Kimelberg HK. Adenosine receptor mediated stimulation of intracellular calcium in acutely isolated astrocytes. Brain Research. 1998; 798:294–303. [PubMed: 9666151]

36. Skoff RP, Knapp PE. Division of astroblasts and oligodendroblasts in postnatal rodent brain: evidence for separate astrocyte and oligodendrocyte lineages. Glia. 1991; 4:165–174. [PubMed: 1827776]

37. Soriano E, Del Rio JA, Auladell C. Characterization of the phenotype and birthdates of pyknotic dead cells in the nervous system by a combination of DNA staining and immunohistochemistry for 5'-bromodeoxyuridine and neural antigens. J. Histochem. Cytochem. 1993; 41:819–827. [PubMed: 8315274]

38. Ullian EM, Sapperstein SK, Christopherson KS, Barres BA. Control of Synapse Number by Glia. Science. 2001; 291:657–661. [PubMed: 11158678]

39. Wagner B, Natarajan A, Grunaug S, Kroismayr R, Wagner EF, Sibilia M. Neuronal survival depends on EGFR signaling in cortical but not midbrain astrocytes. The EMBO journal. 2006; 25:752–762. [PubMed: 16467848]

40. Zhou Q, Petersen CC, Nicoll RA. Effects of reduced vesicular filling on synaptic transmission in rat hippocampal neurones. The Journal of physiology. 2000; 525(Pt 1):195–206. [PubMed: 10811737]

41. Zong H, Espinosa JS, Su HH, Muzumdar MD, Luo L. Mosaic Analysis with Double Markers in Mice. Cell. 2005; 121:479–492. [PubMed: 15882628]

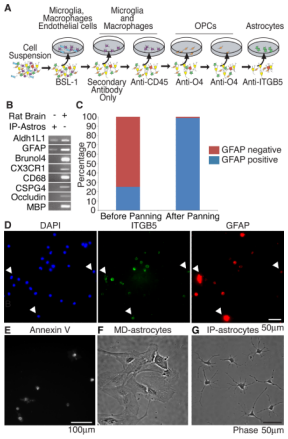

Figure 1. Establishment of an immunopanning protocol for rat astrocytes

(A) Cortical suspensions were passed over successive panning plates to remove endothelial cells and microglia (BSL-1), microglia and macrophages (secondary only plate), microglia (CD45), oligodendrocyte precursor cells (O4) and finally a positive panning plate for astrocytes (ITGB5). **(B)** Purity of IP-astrocytes validated by RT-PCR and **(C)** immunostaining with GFAP. Before immunopanning, the whole cell brain suspension contained 25.1% GFAP+ cells, after immunopanning, the isolated cells were 98.7% GFAP+. **(D)** ITGB5 was present on all astrocytes. All cells in cortical cell suspensions that were GFAP+ were also ITGB5+ (arrowheads). **(E)** Astrocytes are positive for the apoptotic marker Annexin V. **(F)** MD-astrocytes had flat and fibroblast-like morphologies at 14DIV **(G)** IP-astrocytes cultured with HBEGF for 14DIV were healthy and extended multiple processes.

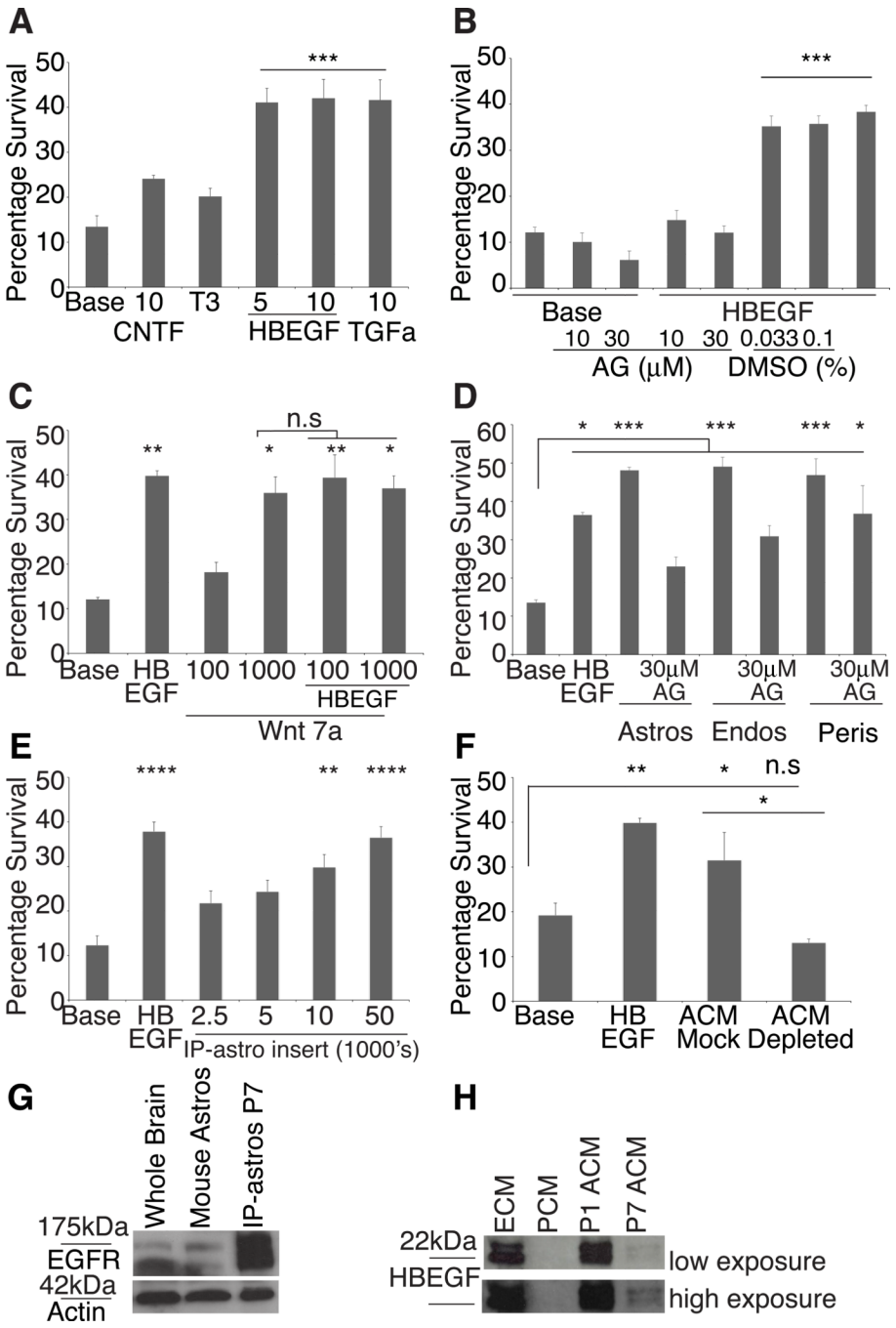

Figure 2. P7 Astrocytes require trophic factors for survival or die by apoptosis

(A) Addition of 5 or 10 ng/ml of HBEGF or 10ng/ml TGFα significantly ($p<0.001$) promoted IP-astrocyte survival. Neither 10ng/ml CNTF nor T3 significantly increased survival of IP-astrocytes. **(B)** AG1478 (AG), did not affect basal survival of astrocytes, but at 10μM and 30μM, significantly inhibited the effect of 5ng/ml HBEGF (HBEGF) not observed in control conditions with DMSO ($p<0.001$). **(C)** 1μg/ml of Wnt7a is a trophic factor for astrocytes (**$p<0.01$), but the effect was not significantly additive with 5ng/ml HBEGF. Values on x-axis are in ng/ml **(D)** Feeder layers of astrocytes, endothelial cells and pericytes produced soluble trophic factors that significantly promoted the survival of astrocytes (***$p<0.001$). 30μM AG1478 (AG) negated the survival-promoting effect of

astrocytes and partially of endothelial cells, but not pericytes (*p<0.05). **(E)** IP-astrocytes P7 grown in inserts at densities higher than 10,000 cells/insert kept IP-astrocytes P7 alive. **(F)** Mock depletion of ACM with goat anti-Gγ13 IgG did not negate the survival-promoting effect of ACM. Depletion of ACM with goat anti-HBEGF IgG negated the survival-promoting effect of ACM. **(G)** Western blot analysis revealed that both mouse astrocytes and rat IP-astrocytes P7 expressed EGFR. **(H)** ECM and P1 ACM contained high levels of HBEGF, P7 ACM contained lower levels and none in PCM. Top blot: low exposure, bottom blot: high exposure. Also see Figure S1

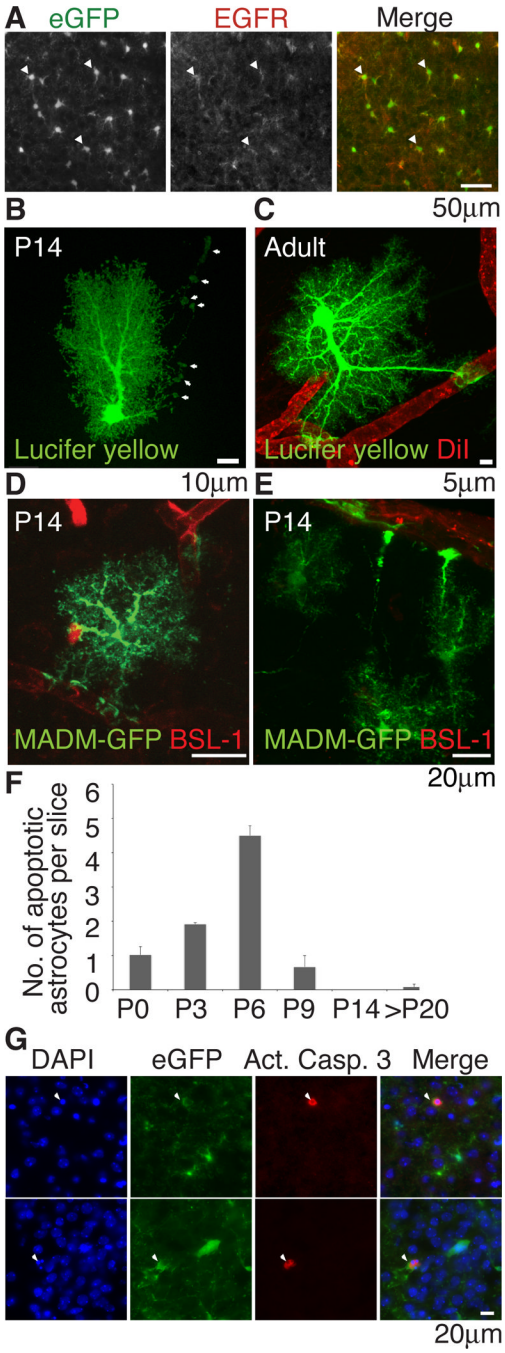

Figure 3. Astrocytes express EGFR, contact blood vessels and die by apoptosis *in vivo*

(A) Immunohistochemical staining for EGFR in P6 Aldh1L1-eGFP mice showed that majority of cortical astrocytes expressed EGFR (white arrowheads=EGFR+,Aldh1L1-eGFP +). **(B,C)** All hippocampal astrocytes at P14 (n=23) and adult (n=22) contacted blood vessels. **(B)** P14 astrocytes send out long processes that contact but not ensheathed blood vessels (white arrows). **(C)** Full ensheathement was observed in the adult. **(D,E)** MADM-labeling sparsely labels astrocytes eGFP+ in the brain. Blood vessels were stained with BSL-1 and eGFP+ astrocytes of the cortex visualized with confocal microscopy. 30 of 31 astrocytes visualized contacted blood vessels **(F,G)** Quantification of immunohistochemical staining with activated caspase 3 (red) in Aldh1L1-eGFP (green) mice and colocalization

with condensed nuclei visualized with DAPI (blue) (arrowheads) revealed that astrocyte apoptosis was observed at P6 **(G)** Immunostaining of apoptotic astrocytes in P6 Aldh1L1-eGFP mice.

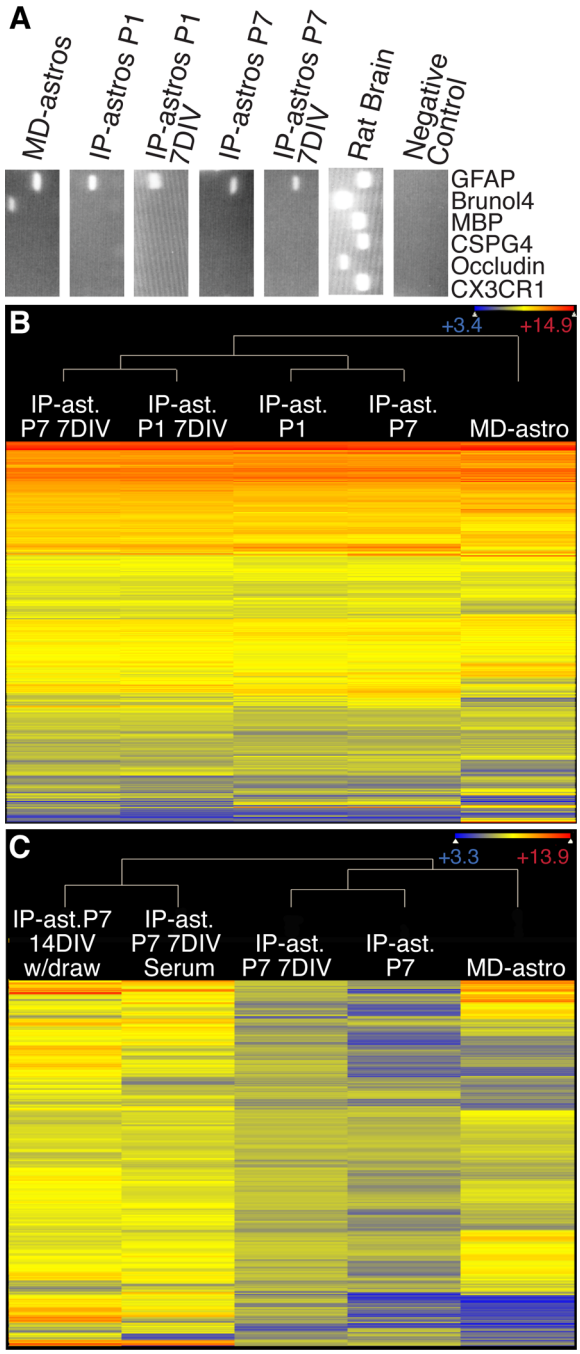

Figure 4. Comparison of IP-astrocyte expression profiles with MD-astrocytes

(A) Purity was assessed by RT-PCR with major cell type markers. MD-astrocytes have neuronal contamination not observed in IP-astrocytes whether acute or cultured. **(B)** Heat map of 15,960 genes where gene expression exceeds 200 in at least one sample. Acutely isolated IP-astrocytes at P1 and P7 (IP-ast P1, P7), IP-astrocytes that have been cultured in HBEGF for 7 days (IP-ast P1, P7 7DIV) and MD-astrocytes gene expression was normalized and plotted on a $\log_2$ color scale. Cooler colors represent low expression and warm colors the converse. MD-astrocytes profiles are distinct from IP-astrocytes and cultured IP-astrocytes are closer in their profiles to their acutely isolated counterparts. **(C)** Heat map showing expression levels of 365 serum-induced genes across samples. IP-

Astrocytes P7 were treated for 7d immediately after isolation with 10% serum and either processed for RNA (IP-ast P7 7DIV Serum) or the serum withdrawn and cells cultured for an additional 7d (IP-ast P7 14DIV w/draw) and compared to IP-ast. P7 7DIV cultured in base media with HBEGF, acutely isolated IP-ast P7 and MD-astrocytes. Serum induction did not cause IP-astrocytes to exhibit a profile like MD-Astrocytes and serum withdrawal did not cause reversion of the serum-induced genes. Also see Tables S1–5.

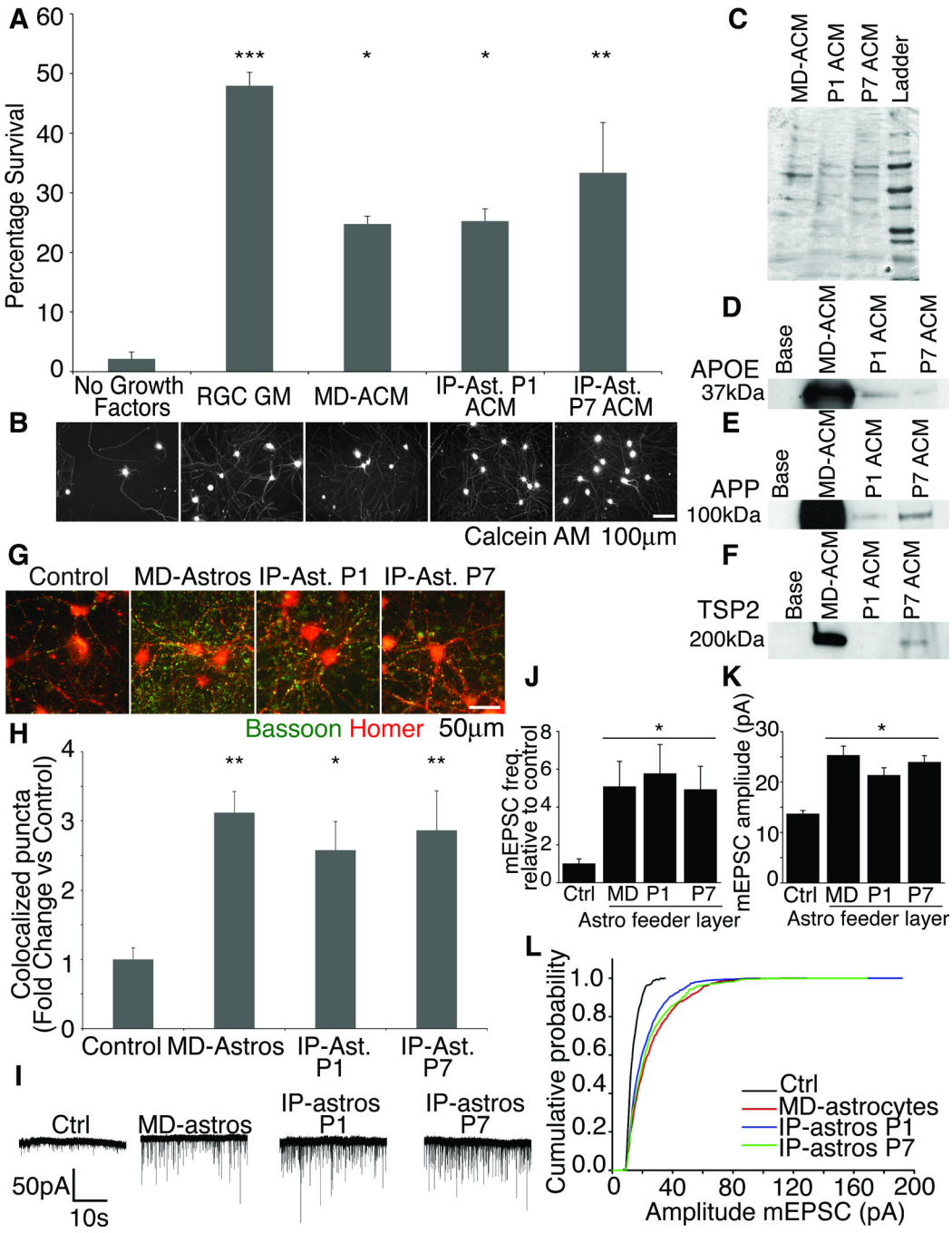

Figure 5. IP-astrocytes in culture retained functional properties

(A,B) IP-astrocyte ACM was as capable of keeping neurons alive as MD-astrocytes was. The neurons were healthy and extended multiple processes. Majority of neurons died in the absence of trophic support. ACM derived from IP-astrocytes P1 and P7 (IP-ast P1 and P7 ACM), MD-astrocytes (MD-ACM) and a positive control of RGC growth media was used. **(C)** Coomassie gel of ACM used to ensure equivalent protein loading. **(D)** MD-astrocytes produced much higher levels of APOE **(D)**, APP **(E)** and TSP2 **(F)**, compared to P1 and P7 ACM. P1 ACM did not contain detectable levels of TSP2. **(G)** Synaptogenesis was quantified by assessing colocalization of presynaptic marker bassoon (green) and postsynaptic marker homer (red) with ImageJ. (**H**) IP-ast P1 and P7 feeder layers were as

effective at inducing structural synapses as MD-astrocytes were. Without an astrocyte feeder layer, few synapses were observed (control) (**p<0.01,*p<0.05) **(I)** Sample traces of whole-cell patch clamp recordings from RGCs made in the presence of TTX. Few mEPSCs were observed without feeder layer of astrocytes (Ctrl). **(J)** Frequency and amplitude of mEPSCs recorded increased significantly with MD-astrocytes, IP-astros P1 or P7 feeder layers ($p < 0.05$). **(L)** IP-astros P1 and P7 caused a shift in cumulative amplitude of mEPSCs to a similar level as MD-astrocytes.

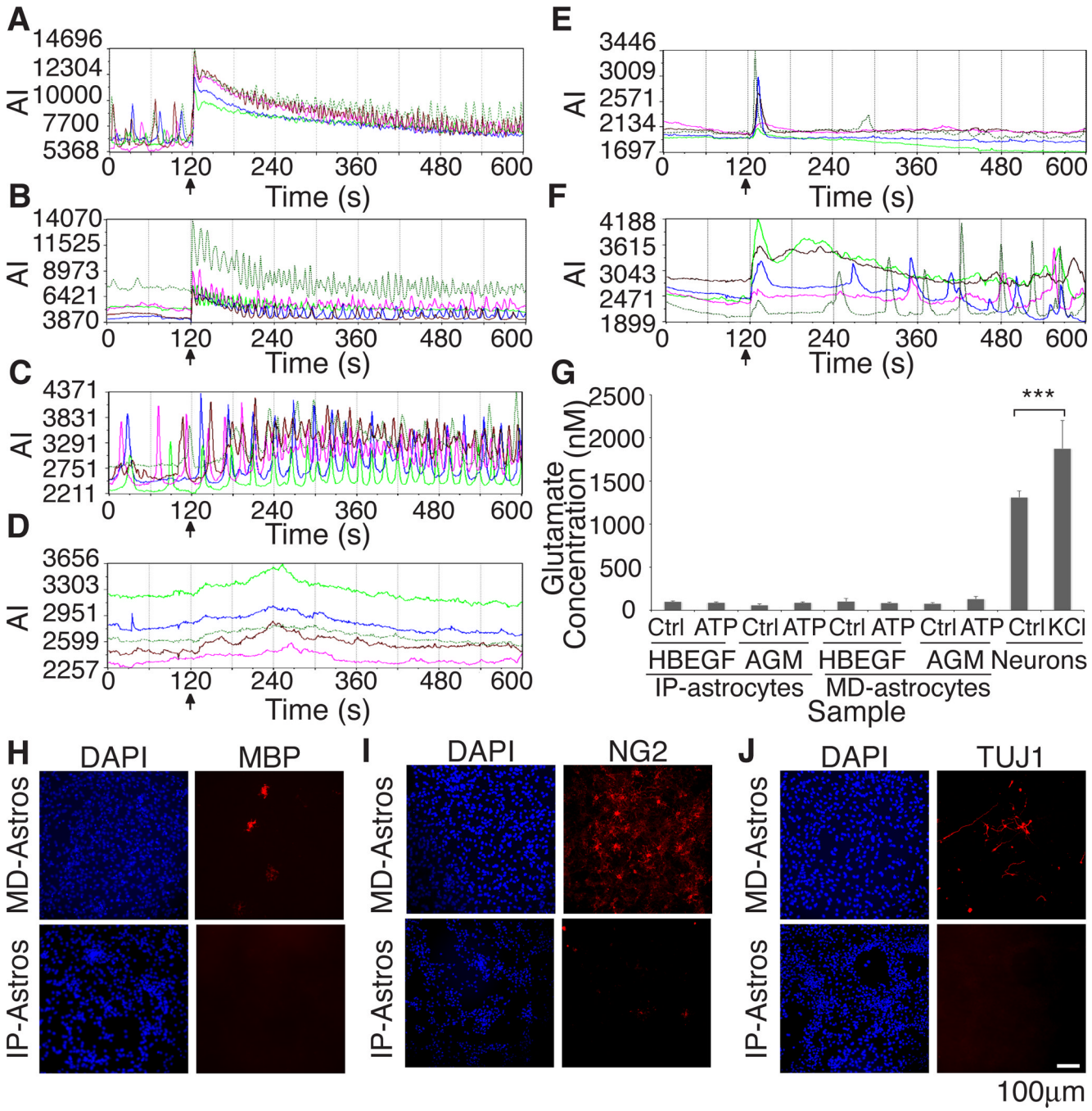

Figure 6. Calcium responses to different stimuli differ between MD-astrocytes and IP-astrocytes and MD-astrocytes are contaminated with several cell types

Astrocytes do not exhibit glutamate release in response to ATP *in vitro* (A–F) Stimuli was added at 120s (black arrow). Graphs of calcium responses from 5 different cells. Graph axes are average intensity (AI, arbitrary units) vs time (s) **(A)** Both MD-astrocytes and **(B)** IP-astrocytes P7 responded to ATP with increased calcium oscillations. **(C)** MD-astrocytes responded (83.4±4.4%, n=118, p<0.0001) robustly to 50mM KCl with increased frequency of oscillations. **(D)** No calcium response was observed with KCl addition in IP-astrocyte cultures. **(E)** No response of cells due to media addition was observed in IP-astrocytes treated with 10% serum for 4 days. **(F)** Cultured IP-astrocytes treated with 10% serum

caused a significant number of astrocytes to respond to KCl (53.3±7.4%, n=209, $p<0.001$). **(G)** Glutamate was readily released by neurons with KCl stimulation (***$p<0.001$). Release was not detected in IP nor MD-astrocytes treated with HBEGF or MD-astrocyte growth media (AGM,10% serum) in response to 100μM ATP. **(H–J)** MD-astrocyte cultures were contaminated with oligodendrocytes (MBP), OPCs and pericytes (NG2) and neurons (TUJ1) whereas minimal contamination was observed in cultures of IP-astrocytes. Also see Figure S2.

Table 1

Comparison of number of genes that differ between acute, cultured IPastrocytes and MD-astrocytes

Fewer differences exist between acutely isolated astrocytes (IP-ast P1 and P7) and their cultured counterparts cultured for 7DIV (IP-ast P1 and P7 7DIV) than MD-astrocytes.

	No of Genes			
	IP- ast P7 vs MD-astros	**IP-ast P1 vs MD-astros**	**IP-ast P7 vs IP-ast P7 7DIV**	**IP-ast P1 vs IP-ast P1 7DIV**
$p < 0.05$	729	547	54	118
$P < 0.001$	369	254	21	45
8-fold change and $p < 0.05$	432	300	41	48
8-fold change and $p < 0.001$	290	195	21	45

Table 2

Top 30 genes induced by serum in IP-astrocyte P7

IP-astrocytes P7 cells were treated with 10% serum for 7 days and either processed for total RNA (IP-ast P7 7DIV serum) or the media exchanged for HBEGF without serum for an additional 7 days (IP-ast P7 14DIV w/draw). Gene expression was compared to MD-astrocytes, acutely isolated P7 (IP-ast P7) cells and P7 cells cultured for 7d in HBEGF (IP-ast P7 7DIV). 13/30 genes induced by serum were not expressed by MD-astrocytes and only 17/30 were more than moderately expressed (>200). Reversion of gene expression levels to baseline levels did not occur after serum withdrawal.

No.	Probe Set ID	Gene	Gene Title	MD -Astros	IP-ast P7 7 DIV Serum (A)	IP-ast P7 14 DIV w/draw	IP-ast P7 7DIV	IP-ast P7 (B)	Fold Change of A/B
1	1372011_at			1898	1893	1568	126	21	91
2	1370019_at	Sult1a1	sulfotransferase family,cytosolic,1A,phenol-preferring,member1	358	5715	11358	551	73	78
3	1367661_at	S100a6	S100 calcium binding protein A6	14339	13447	11898	4368	172	78
4	1370973_at	Scn7a	sodium channel, voltage-gated, type VII, alpha	398	3895	6137	3325	59	66
5	1376311_at	Ntng1	netrin G1	1073	1143	317	83	18	64
6	1387659_at	Gda	guanine deaminase	2251	2821	2652	149	51	55
7	1393696_at	Fibin	fin bud initiation factor homolog (zebrafish)	30	1138	1330	97	24	48
8	1368420_at	Cp	ceruloplasmin	437	3194	8813	587	72	44
9	1372219_at	Tpm2	tropomyosin 2, beta	2157	4922	3119	978	126	39
10	1390024_at			348	4110	7582	947	107	38
11	1372599_at	Mgst2	microsomal glutathione S-transferase 2	581	1194	861	256	32	38
12	1370952_at	Gstm2	glutathione S-transferase mu 2	213	2530	3986	283	71	36
13	1383875_at	Upk1b	uroplakin 1B	29	750	684	181	21	35
14	1379584_at			267	519	220	40	15	34
15	1370902_at	Akr1b8	aldo-keto reductase family 1, member B8	121	943	130	164	28	34
16	1367592_at	Tnnt2	troponin T type 2 (cardiac)	91	1217	4746	249	37	33
17	1373628_at			82	2539	771	349	82	31
18	1391450_at	Loxl2	lysyl oxidase-like 2	724	1478	474	225	49	30
19	1384707_at	Scara5	scavenger receptor class A, member 5 (putative)	21	1056	1467	133	37	29
20	1368014_at	Ptges	prostaglandin E synthase	62	1183	279	45	42	28
21	1374284_at	Rassf4	Ras association(RalGDS/AF-6)domain family member4	3327	2743	1455	1255	98	28
22	1383916_at	Tbx15	T-box 15	19	1223	1207	265	45	27
23	1383456_at			18	658	437	102	21	27
24	1374172_at	Col8a2	collagen, type VIII, alpha 2	121	4376	4359	1628	166	26

Neuron. Author manuscript; available in PMC 2012 September 8.

No.	Probe Set ID	Gene	Gene Title	MD -Astros	IP-ast P7 7 DIV Serum (A)	IP-ast P7 14 DIV w/draw	IP-ast P7 7DIV	IP-ast P7 (B)	Fold Change of A/B
25	1368868_at	Akap12A	kinase (PRKA) anchor protein 12	1863	2409	854	227	92	26
26	1373727_at	Fibin	fin bud initiation factor homolog (zebrafish)	107	1573	2580	230	62	26
27	1374477_at	Prrx2	paired related homeobox 2	96	1496	708	229	59	25
28	1369074_at	Slc38a4	solute carrier family 38, member 4	12	540	136	71	22	25
29	1368171_at	Lox	lysyl oxidase	4727	4537	3651	698	186	24
30	1393891_at	Col8a1	collagen, type VIII, alpha 1	152	2865	723	373	119	24